

Article

Analysis of Resonance Asymmetry Phenomenon in Resonant Fiber Optic Gyro

Zhuoyan Li ^{1,2}, Nie He ^{1,2}, Xuqiang Sun ², Chao Jin ², Chengxiang Liu ^{3,*} and Xu Wu ^{1,3,*} 

¹ Sino-German College for Intelligent Manufacturing, Shenzhen Technology University, Shenzhen 518060, China

² Guangdong Provincial Key Laboratory of Micro/Nano Optomechatronics Engineering, College of Optoelectronic Engineering, Shenzhen University, Shenzhen 518060, China; 2160190403@email.szu.edu.cn (Z.L.); 2160190401@email.szu.edu.cn (N.H.); 2150190122@email.szu.edu.cn (X.S.); 2151190215@email.szu.edu.cn (C.J.)

³ Guangdong Provincial Key Laboratory of Micro/Nano Optomechatronics Engineering, College of Mechatronics and Control Engineering, Shenzhen University, Shenzhen 518060, China

* Correspondence: chxliu@szu.edu.cn (C.L.); xwu@szu.edu.cn (X.W.); Tel.: +86-158-8950-3543 (X.W.)

Received: 14 January 2018; Accepted: 17 February 2018; Published: 26 February 2018

Abstract: This experiment demonstrated the resonance asymmetry phenomenon in the resonant fiber optic gyro. The asymmetry of resonant curve affects the system open-loop bias and its stability, which directly affects the accuracy of angular velocity measurement. In this paper, a new mathematic model is established. The influence of the coupler normal mode loss difference (the phase difference between the coupler cross port output optical field and direct port is less than the ideal $\pi/2$) on the symmetry of resonant curve, the resonant signal modulated by the triangular wave, and the demodulation curve are analyzed. Moreover, the asymmetry of the resonant curve leads to the asymmetry of the resonant signal, as modulated by the triangular wave and the demodulation curve from the theoretical simulation and the experiment.

Keywords: resonant fiber optic gyro; normal mode loss difference; resonance asymmetry

1. Introduction

Gyro is an inertial sensor for the rotation rate measurement [1]. At present, fiber optic gyro, micro-optic gyro, laser gyro has great development potential because of its own advantages [1–8]. Resonant fiber optic gyro (RFOG) based on the Sagnac effect has the advantages of high sensitivity and large dynamic range [2]. When compared with the traditional interferometric fiber optic gyro (IFOG), RFOG can achieve the same detection precision as IFOG with a much shorter fiber length, which gives evident superiority in the further integration, as well as improves its application value in the fields of navigation, aerospace, defense industries, and guidance systems [1–9].

RFOG is a kind of high-precision angular velocity sensor based on the optical Sagnac effect. It can detect the angular velocity information of the gyroscopic rotation by detecting the resonance frequency difference of the clockwise (CW) and counterclockwise (CCW) light waves that are caused by rotation. However, the optical Sagnac effect has an extremely weak effect in a RFOG system. The working frequency of the laser is as high as 193 THz. When the diameter of the optical fiber resonant ring of the RFOG system is 15 cm and the rotational angular velocity is 1 deg/s, the resonant frequency difference caused by rotation is only 116 Hz. Thus, detecting the signal of several hundred Hz at such a high working frequency is very difficult. Meanwhile, when the external environment, including temperature and stress changes, the laser's center frequency and the resonant frequency of the fiber ring resonator (FRR) will also change. Therefore, directly measuring the resonance frequency difference of the CW and CCW light waves caused by the rotation using the RFOG system is extremely difficult; in addition,

appropriate modulation and demodulation techniques are needed to improve the sensitivity of the signal detection system [9]. In a single closed-loop RFOG system, the triangular wave modulated signals with different frequencies are used to modulate the CW and CCW light waves. One of the light waves is processed by a field-programmable gate array (FPGA) based digital detection control circuit, whereas the FPGA output feedback signal controls the center frequency of the laser. Thus, the laser is locked into the resonant frequency of this light wave. Afterward, the demodulation curve of the output signal of the other light wave will reflect the resonant frequency difference of the two light waves to achieve the angular velocity measurement. If the resonant curve is asymmetric, the demodulation curve is asymmetric, which will result in the laser's center frequency being unable to be locked to the resonance frequency of one of the light waves. Thus, this phenomenon affects the system open-loop bias and its stability, which directly affects the angular velocity measurement accuracy.

Stokes et al. reported a FRR composed of a single mode fiber for the first time in 1982 and found the resonance asymmetry in the resonant curve measurement [10]. They also explained and analyzed the resonant curve asymmetry in 1983 [2]. The normal mode loss difference of the coupler will result in the phase difference between the coupler cross port output optical field and the direct port is less than the ideal $\pi/2$. Thus, the resonant curve appears asymmetric phenomenon [10,11]. R. Carroll found that the phase difference between the cross port output optical field and the direct port in the coupler with low/high coupling coefficients is different from $\pi/2$. To form a high-resolution resonator, using coupler with low/high coupling coefficients is necessary [12]. A coupler with low/high coupling coefficients can also be used into a FRR of the resonant fiber optical gyro; thus, the phase difference between the coupler cross port output optical field and direct port is less than the ideal $\pi/2$, resulting in the asymmetry phenomenon of the resonant curve. Zhejiang University has also conducted an in-depth study on the asymmetry phenomenon of the resonant curve due to the normal mode loss difference of the coupler [13]. In a RFOG, the coupler factor is not the only factor that causes the asymmetry phenomenon of the resonant curve. Polarization fluctuations [14], optical Kerr effect [15], FRR ambient temperature fluctuations [16], backscattering [17], and other factors can cause the resonant curve to be asymmetric. However, the phase difference between the coupler cross port output optical field and direct port is less than the ideal $\pi/2$, which is the most important factor affecting the asymmetry of the resonant curve [13].

In this paper, a new mathematic model is established. The influence of the normal mode loss difference of the coupler (the phase difference between the coupler cross port output optical field and direct port is less than the ideal $\pi/2$) on the symmetry of the resonant curve, the resonant signal modulated by the triangular wave, and the demodulation curve are all analyzed in detail. At the same time, the asymmetry of the resonant curve will lead to the asymmetry of the resonant signal modulated by the triangular wave and the demodulation curve from the theoretical simulation and the experiment.

2. System Structure of Resonant Fiber Optic Gyro

RFOG system structure is depicted in Figure 1. The laser light emitted by a narrow-line-width semiconductor laser is divided into two equal power beams by a 50:50 coupler C1 after passing through an isolator. The two light beams passed through the LiNbO₃ phase modulator (PM)1 and PM2, respectively, which are modulated by the modulated signals of different frequencies. Afterwards, the two beams are incident to the FRR through the circulators (CIR), namely, CIR1 and CIR2, in the CCW and CW directions, respectively. C2 is the coupler connected to the FRR. Finally, the two light beams are output to photodiode (PD) 2 and PD1 via CIR2 and CIR1, respectively. Among the light waves, the CW light wave is processed by the FPGA-based digital detection control circuit. Afterward, the FPGA output feedback signals to control the center frequency of laser; thus, the laser is locked into the resonant frequency of the CW light wave. At this moment, the output optical signal of the CCW light wave can reflect the resonance frequency difference of the CW and CCW light waves. Moreover, the rotational angular speed can be obtained after being processed by FPGA.

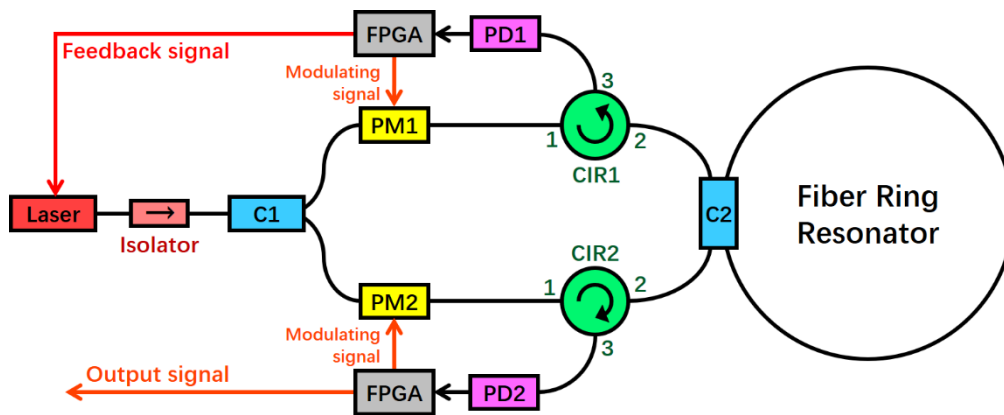


Figure 1. System structure of RFOG. (FPGA: field-programmable gate array, PD: photodiode, PM: phase modulator, C: coupler, and CIR: circulator).

3. Model Establishment and Simulation Results

3.1. Resonant Curve

The transmission process of one of the light waves in the FRR is depicted in Figure 2a. The incident light wave is divided into two beams from the Port 1 through the coupler. A light wave is directly output from Port 4, whereas the other light wave enters the FRR from Port 3. After propagating a circle, the light wave enters the coupler again through Port 2. A part of the light wave is output through Port 4, while the remaining part of the light wave enters the FRR again from Port 3 and continues to propagate in the cavity. Using analogy, when the light wave propagates one circle into the resonator, a part of the light wave is output from Port 4 of the coupler C2, and the light waves output from Port 4 are superposed on each other. Multiple beam interference occurs. Moreover, the optical field complex amplitude and the light intensity of Port 4 are the results of multiple beam interference. If the optical field complex amplitude of port i is denoted by E_i (where $i = 1, 2, 3, 4$), then the ratio of the optical field complex amplitude of Port 4 to the incident light is E_4/E_1 , while the ratio of the light intensity of Port 4 to the incident light is $|E_4/E_1|^2$.

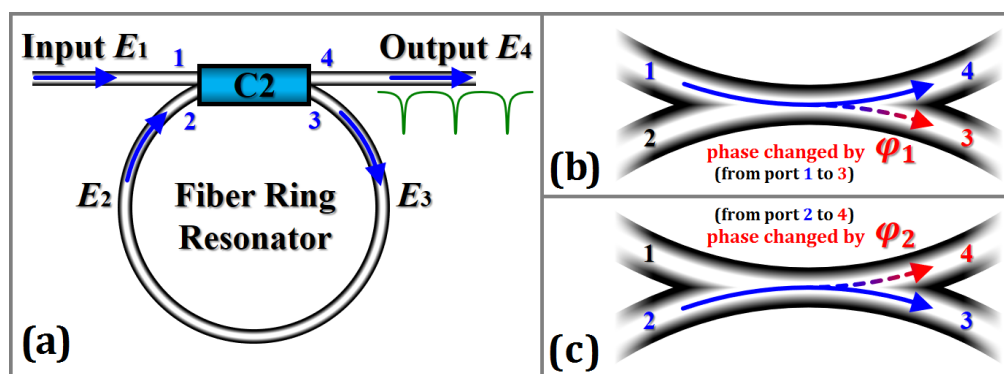


Figure 2. (a) Transmission process of one of the light waves in FRR. (b) The phase is changed by φ_1 from port 1 to 3. (c) The phase is changed by φ_2 from port 2 to 4. (E_i : the optical field complex amplitude of port i is denoted).

If the light passes through the cross port of the coupler C2, the phase changes by $\pi/2$. When the light wave passes through the cross port to reach the inside of FRR or passes through the cross port to reach the outside of FRR, the phases both change by $\pi/2$. Multiple beam interference occurs among the light waves arriving at Port 4 through the direct port and the light in the FRR that is constantly coupled

to Port 4. Only when the light satisfies a certain optical frequency, then it can result to the resonance phenomenon. Furthermore, the output curve of Port 4 presents a downward depression (power is 0 or small). Thus, if $|E_4/E_1|^2$ takes a minimum value, then it meets the FRR resonance conditions.

However, if the light wave passes through the cross port of coupler C2, the phase change is less than the ideal $\pi/2$. To further discuss the effect of the phase difference between the output optical field of the coupler cross port and the direct port being less than the ideal $\pi/2$ on the output optical power, we need to analyze the simultaneous equations satisfied by the optical field of each port and solve the ratio of the optical field complex amplitude of Port 4 to the incident light E_4/E_1 and the ratio of the light intensity of Port 4 to the incident light $|E_4/E_1|^2$. As shown in Figure 2b, c, the light phase from Port 1 to Port 3 is changed by φ_1 , and the light phase from Port 2 to Port 4 is changed by φ_2 . The optical power coupling ratio between the coupler direct port and cross port is $k:(1-k)$. The remaining percentages of the optical power that is caused by insertion loss of the coupler and transmission loss of the fiber ring are ρ_c and ρ_L , respectively. The light wave frequency entering the FRR is ν . The time required to enter the ring fiber resonator from Port 3 to propagate 1 circle to reach Port 2 is τ . The q -th resonant frequency is ν_q , that is, $\nu_q = q/\tau$. When the light wave frequency entering the FRR satisfies $\nu = \nu_q$, the light wave resonates in the FRR. Then, the output optical field complex amplitude of each port can be expressed as

$$E_2 = \sqrt{\rho_L} e^{-j2\pi\nu\tau} E_3, \quad (1)$$

$$E_3 = e^{j\varphi_1} \sqrt{(1-k)\rho_c} E_1 + \sqrt{k\rho_c} E_2, \quad (2)$$

$$E_4 = \sqrt{k\rho_c} E_1 + e^{j\varphi_2} \sqrt{(1-k)\rho_c} E_2. \quad (3)$$

Combining Equation (1) to Equation (3), the ratio of the optical field complex amplitude from Port 4 to Port 1 can be expressed as

$$\frac{E_4}{E_1} = \sqrt{k\rho_c} + \frac{e^{j\varphi_0}(1-k)\rho_c}{\sqrt{\rho_L^{-1}e^{j2\pi\nu\tau} - \sqrt{k\rho_c}}}, \quad (4)$$

where $\varphi_0 = \varphi_1 + \varphi_2$. The left and right sides of Equation (4) are modeled and then squared. In addition, the optical power ratio from Port 4 to Port 1 can be expressed as

$$I = \left| \frac{E_4}{E_1} \right|^2 = \rho_c \left[k + (1-k)\sqrt{\rho_c\rho_L} \cdot \frac{2\sqrt{k}\cos(2\pi\nu\tau - \varphi_0) + \sqrt{\rho_c\rho_L}(1-k-2k\cos\varphi_0)}{1 + k\rho_c\rho_L - 2\sqrt{k\rho_c\rho_L}\cos 2\pi\nu\tau} \right], \quad (5)$$

where I is the normalized intensity. If the light passes through the cross port of coupler C2, the phase changes by $\pi/2$, that is, $\varphi_1 = \varphi_2 = \pi/2$. Then, the ratio of the optical field complex amplitude from Port 4 to Port 1 can be expressed as

$$\frac{E_4}{E_1} = \sqrt{k\rho_c} - \frac{(1-k)\rho_c}{\sqrt{\rho_L^{-1}e^{j2\pi\nu\tau} - \sqrt{k\rho_c}}}. \quad (6)$$

Similarly, the left and right sides of Equation (6) are modeled and then squared. The optical power ratio from Port 4 to Port 1 can be expressed as

$$I = \left| \frac{E_4}{E_1} \right|^2 = \rho_c \left[1 - \frac{(1-k)(1-\rho_c\rho_L)}{1 + k\rho_c\rho_L - 2\sqrt{k\rho_c\rho_L}\cos 2\pi\nu\tau} \right]. \quad (7)$$

On the basis of the analysis above on the transmission process of light waves in FRR, the resonant curve can be simulated. The main simulation parameters are as follows: the splitting ratio and insertion

loss of coupler C2 are 95:5 and -0.4 dB, respectively; the FRR transmission loss is -0.2 dB. If the light passes through the cross port of coupler C2, then the phase is changed by $\pi/2$, that is, $\varphi_0 = \pi$. Thus, the resonant curve is a signal with symmetry, as shown in Figure 3a. If the light wave passes through the cross port of coupler C2, then the phase change is less than the ideal $\pi/2$, that is, $\varphi_0 \neq \pi$. Thus, the resonant curve is a signal with asymmetry. Figure 3b–d lists the cases of $\varphi_0 = 0.95\pi$, 0.90π , and 0.85π , respectively. The results showed that the resonant curve is not symmetrical. The reason is that the light passing through the coupler C2 is not orthogonal, and the phase change that is caused by non-orthogonal coupling mode is less than the ideal $\pi/2$, which will directly cause the resonant curve to be asymmetric. Moreover, the degree of asymmetry of the resonant curve is related to the degree of φ_0 that deviates from π . The greater the degree of φ_0 that deviates from π , the greater the degree of asymmetry of the resonant curve.

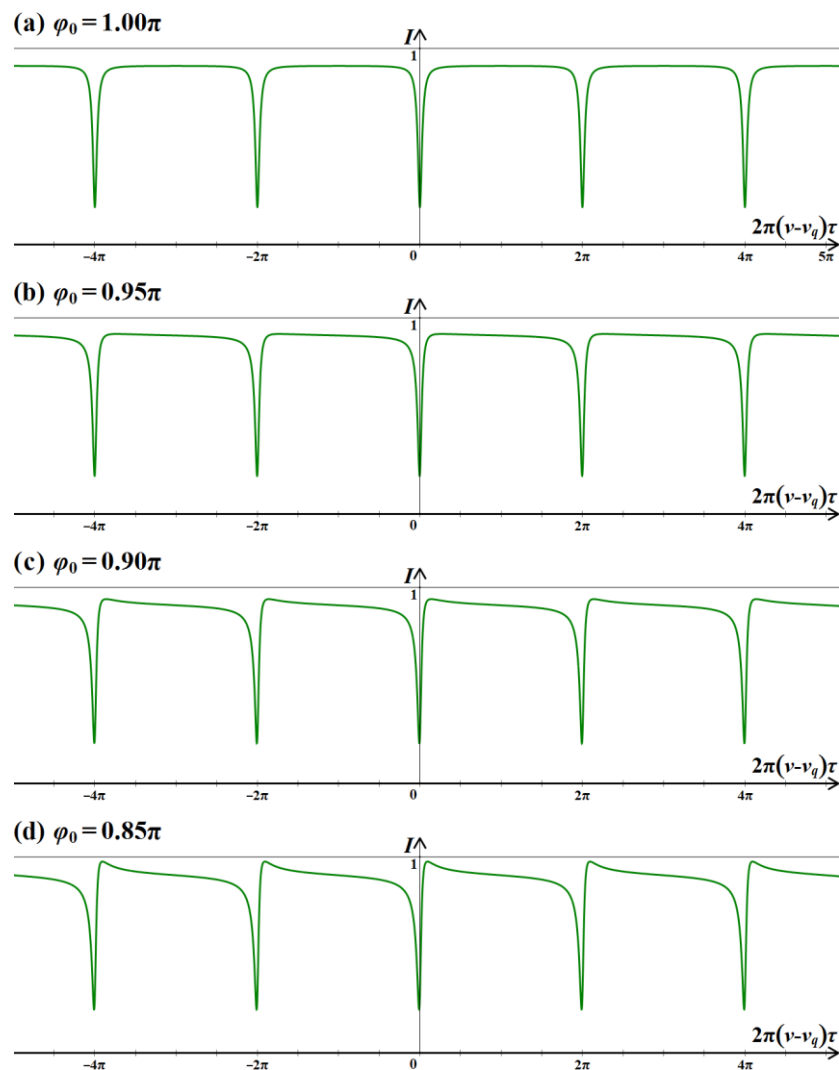


Figure 3. Simulated resonant curve of $\varphi_0 =$ (a) 1.00π , (b) 0.95π , (c) 0.90π , and (d) 0.85π .

3.2. Modulation and Demodulation

Suppose the center frequency of the laser output light wave is ν_L , that is, the center frequency of the light wave that is not modulated is ν_L , and the initial phase is ψ_1 . Then, its complex amplitude can be expressed as

$$E(t) = E_0 e^{j(2\pi\nu_L t + \psi_1)}. \quad (8)$$

The frequency of the light wave incident to the FRR at this time is $\nu = \nu_L$. Suppose the presence of a modulation signal, whose amplitude, frequency, and initial phase are V_p, f and ψ_0 , respectively. This modulation signal is loaded into the phase modulator. Afterward, the light wave is modulated by the phase modulator, $\nu \neq \nu_L$. The complex amplitude of the modulated light wave can be expressed as

$$E(t) = E_0 e^{j[2\pi\nu_L t + \psi_1 + \frac{\pi}{V_\pi} V_p P(2\pi f t + \psi_0)]}, \quad (9)$$

where V_π is the half-wave voltage of the phase modulator, and $P(\cdot)$ is a phase modulation function. When the resonant signal is modulated by the triangular wave,

$$P(x) = \frac{2}{\pi} \arcsin(\sin x). \quad (10)$$

The differential of P is

$$\frac{dP(x)}{dx} = P'(x) = \frac{2}{\pi} \operatorname{sgn}(\cos x), \quad (11)$$

where $\operatorname{sgn}(\cdot)$ is a sign function. The laser's frequency is changed slowly to let ν_L to vary slowly and linearly over time t . The complex amplitude of the light wave that has been modulated can be expressed as

$$E(t) = E_0 e^{j[2\pi \int \nu_L(t) dt + \frac{\pi}{V_\pi} V_p P(2\pi f t + \psi_0)]}. \quad (12)$$

The frequency ν of the light wave incident to the FRR at this time can be expressed as

$$\nu = \frac{1}{2\pi} \cdot \frac{d}{dt} \left[2\pi \int \nu_L(t) dt + \frac{\pi}{V_\pi} V_p P(2\pi f t + \psi_0) \right] = \nu_L(t) + \frac{\pi}{V_\pi} V_p f P'(2\pi f t + \psi_0). \quad (13)$$

Combining Equations (13) and (5), the optical power ratio of Port 4 to Port 1 can be expressed as

$$I = \left| \frac{E_4}{E_1} \right|^2 = \rho_c \left\{ k + (1-k) \sqrt{\rho_c \rho_L} \cdot \frac{2\sqrt{k} \cos \left\{ 2\pi \left[\nu_L(t) + \frac{\pi}{V_\pi} V_p f P'(2\pi f t + \psi_0) \right] \tau - \varphi_0 \right\} + \sqrt{\rho_c \rho_L} (1-k-2k \cos \varphi_0)}{1+k\rho_c\rho_L-2\sqrt{k\rho_c\rho_L} \cos \left\{ 2\pi \left[\nu_L(t) + \frac{\pi}{V_\pi} V_p f P'(2\pi f t + \psi_0) \right] \tau \right\}} \right\}. \quad (14)$$

Equation (14) represents the expression that is satisfied by the phase-modulated resonant signal. By substituting Equation (11) into Equation (14), we can obtain the expression that is satisfied by the resonant signal modulated triangular wave, as follows:

$$\begin{aligned} I|_{\nu=\nu_L(t)+\frac{2}{V_\pi}V_p f \operatorname{sgn}[\cos(2\pi f t+\psi_0)]} \\ = \rho_c \left\{ k + (1-k) \sqrt{\rho_c \rho_L} \cdot \frac{2\sqrt{k} \cos \left\{ 2\pi \left\{ \nu_L(t) + \frac{2}{V_\pi} V_p f \operatorname{sgn}[\cos(2\pi f t + \psi_0)] \right\} \tau - \varphi_0 \right\} + \sqrt{\rho_c \rho_L} (1-k-2k \cos \varphi_0)}{1+k\rho_c\rho_L-2\sqrt{k\rho_c\rho_L} \cos \left\{ 2\pi \left\{ \nu_L(t) + \frac{2}{V_\pi} V_p f \operatorname{sgn}[\cos(2\pi f t + \psi_0)] \right\} \tau \right\}} \right\}. \end{aligned} \quad (15)$$

When the resonant signal is modulated by the triangular wave, then $P'(x) = 2/\pi \cdot \operatorname{sgn}(\cos(x)) = \pm 2/\pi$. From Equation (13), ν is fluctuating $\pm 2V_p f / V_\pi$ on the basis of $\nu_L(t)$. The demodulation curve is the difference between $I(\nu = \nu_L(t) + 2V_p f / V_\pi)$ and $I(\nu = \nu_L(t) - 2V_p f / V_\pi)$. The corresponding expression of the demodulation curve can be expressed as

$$\begin{aligned} D(t) &= I|_{\nu=\nu_L(t)+2V_p f/V_\pi} - I|_{\nu=\nu_L(t)-2V_p f/V_\pi} \\ &= (1-k) \rho_c \sqrt{\rho_c \rho_L} \cdot \left\{ \frac{2\sqrt{k} \cos \left[2\pi \left(\nu_L(t) + \frac{2}{V_\pi} V_p f \right) \tau - \varphi_0 \right] + \sqrt{\rho_c \rho_L} (1-k-2k \cos \varphi_0)}{1+k\rho_c\rho_L-2\sqrt{k\rho_c\rho_L} \cos \left[2\pi \left(\nu_L(t) + \frac{2}{V_\pi} V_p f \right) \tau \right]} \right. \\ &\quad \left. - \frac{2\sqrt{k} \cos \left[2\pi \left(\nu_L(t) - \frac{2}{V_\pi} V_p f \right) \tau - \varphi_0 \right] + \sqrt{\rho_c \rho_L} (1-k-2k \cos \varphi_0)}{1+k\rho_c\rho_L-2\sqrt{k\rho_c\rho_L} \cos \left[2\pi \left(\nu_L(t) - \frac{2}{V_\pi} V_p f \right) \tau \right]} \right\}. \end{aligned} \quad (16)$$

On the basis of the analysis above on the modulation and demodulation process, the resonant signal modulated by the triangular wave and the corresponding demodulation curve can be simulated. As shown in Figure 4, if the light passes through the cross port of coupler C2, then the phase is changed

by $\pi/2$, that is, $\varphi_0 = \pi$. Thus, the resonant curve is a signal with symmetry. According to Equation (7), when $\nu = \nu_q$, $\cos 2\pi\nu\tau$ takes the maximum value of 1, while $|E_4/E_1|^2$ can get the minimum value. At the same time, the resonant signal modulated by the triangular wave and the corresponding demodulation curve are symmetrical. The abscissa O_1 of the resonant frequency, the abscissa A_1 of the lowest point of the resonant curve, and the abscissa B_1 of the zero point of the demodulation curve completely coincide with each other. The linear region of the demodulation curve $|C_{11}C_{12}|$ is also symmetrical, that is, $|C_{11}B_1| = |B_1C_{12}|$. The center frequency of the laser is finally locked at the zero point of the demodulation curve. Thus, the center frequency of the laser can be accurately locked at the resonant frequency of the light wave. As shown in Figure 5, if the light wave passes through the cross port of coupler C2, then the phase change is less than the ideal $\pi/2$, that is, $\varphi_0 \neq \pi$. Supposing that $\varphi_0 = 0.9\pi$, then the resonant curve is a signal with asymmetry. At the same time, the resonant signal modulated by the triangular wave and the corresponding demodulation curve are asymmetrical. According to Equation (5), when $\nu = \nu_q$, $|E_4/E_1|^2$ cannot get the minimum value. The abscissa O_2 of the resonant frequency, the abscissa A_2 of the lowest point of the resonant curve, and the abscissa B_2 of the zero point of the demodulation curve cannot coincide with each other. The linear region of the demodulation curve $|C_{21}C_{22}|$ is also asymmetrical, that is, $|C_{21}B_2| \neq |B_2C_{22}|$. Therefore, the central frequency of the laser cannot be accurately locked into the resonant frequency of the light wave, which affects the system open-loop bias and its stability and directly affects the angular velocity measurement accuracy.

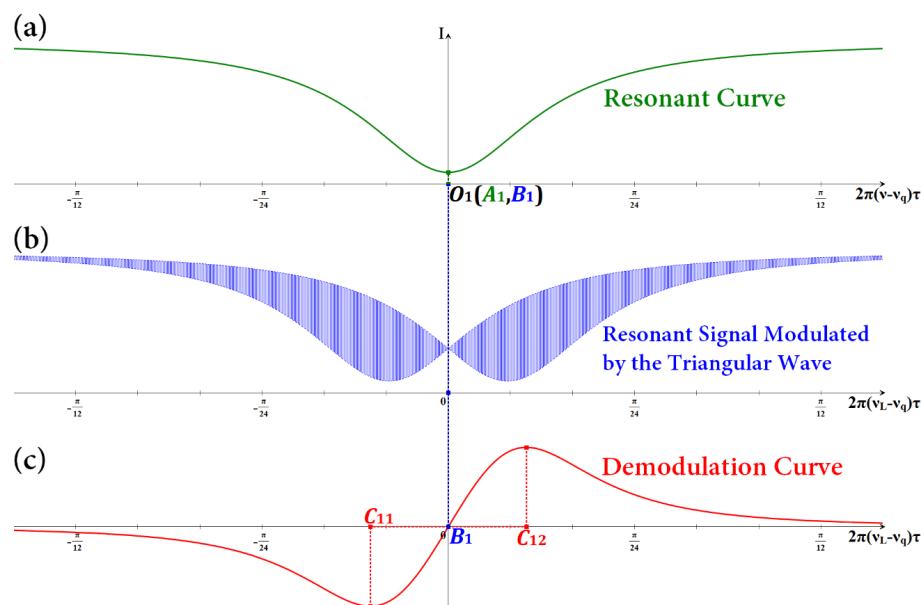


Figure 4. When $\varphi_0 = \pi$, (a) simulated resonant curve, (b) simulated resonant signal modulated by the triangular wave, and (c) simulated demodulation curve.

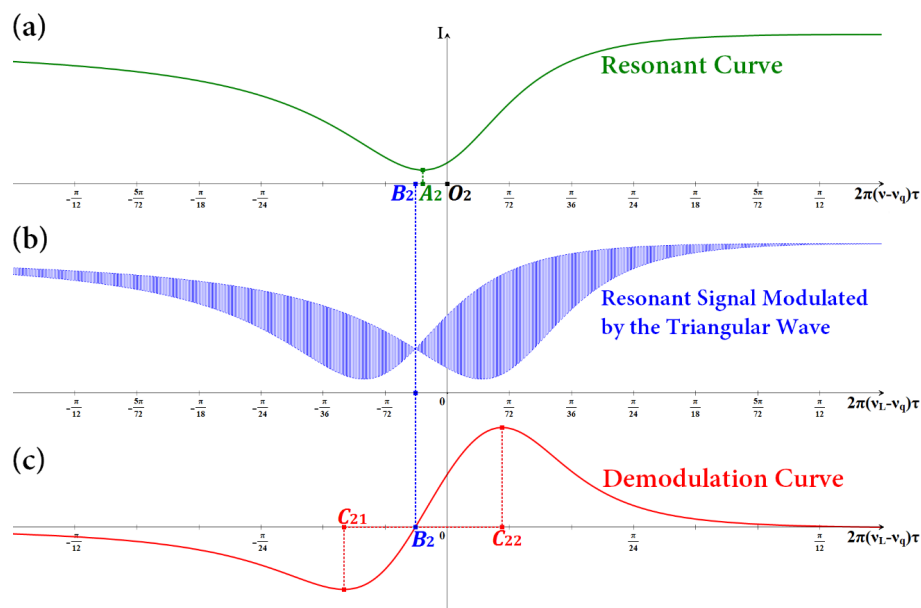


Figure 5. When $\varphi_0 = 0.9\pi$, (a) simulated resonant curve, (b) simulated resonant signal modulated by the triangular wave, and (c) simulated demodulation curve can be obtained.

4. Experimental Results and Discussion

As shown in Figure 1, we set up a RFOG system. To conduct a comparative experiment, we only change the coupler C2 connected to the FRR, while keeping the rest of the components of the RFOG system unchanged. We chose the couplers C2_{#1} and C2_{#2} from two different companies. The basic parameters of both couplers in the test sheet are similar. However, the normal mode loss difference of the coupler in the test sheets is not mentioned. A triangular wave with a frequency of 1 Hz and a peak-to-peak value of 1 V is produced by an arbitrary waveform generator to slowly change the frequency of the narrow linewidth semiconductor laser. The resonant curve observed from the oscilloscope when the coupler connected to the FRR is C2_{#1} is shown in Figure 6a. The asymmetry phenomenon in the experiment almost completely agrees with the asymmetry phenomenon shown in Figure 3b–d of the simulation results. We hypothesize that the asymmetry of this resonant curve is mainly caused by the normal mode loss difference of the coupler. Thus, we replace the coupler C2_{#1} connected with the FRR with the coupler C2_{#2}, which solves the resonant curve asymmetry. The resonant curve that is observed from the oscilloscope is shown in Figure 6b. Thus, the resonant curve is a symmetrical signal. The experimental result is almost completely consistent with simulation result shown in Figure 3a.

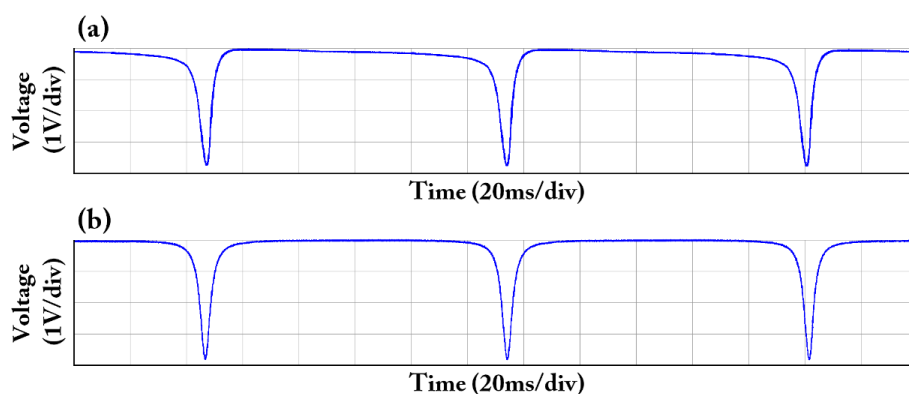


Figure 6. Measured resonant curve of the two different couplers connected to FRR. (a) C2_{#1}; (b) C2_{#2}.

The resonant curve, resonant signal modulated by the triangular wave, and the corresponding demodulation curve observed from the oscilloscope when the coupler connected to FRR is $C2_{\#1}$ are shown in Figure 7. Thus, the resonant curve is a signal with asymmetry. At the same time, the resonant signal modulated by the triangular wave and the corresponding demodulation curve are asymmetrical. The abscissa A_2' of the lowest point of the resonant curve and the abscissa B_2' of the zero point of the demodulation curve cannot coincide with each other. The linear region of the demodulation curve $|C_{21}'C_{22}'|$ is also asymmetrical, that is, $|C_{21}'B_2'| \neq |B_2'C_{22}'|$. Therefore, the central frequency of the laser cannot be accurately locked into the resonant frequency of the light wave, which affects the system open-loop bias and its stability, and directly affects the accuracy of the angular velocity measurement. The asymmetry phenomenon in the experiment almost completely agrees with the asymmetry phenomenon shown in Figure 5 of the simulation results. The resonant curve, the resonant signal modulated by the triangular wave and the corresponding demodulation curve observed from the oscilloscope after the coupler $C2_{\#1}$ connected with the FRR is changed with the coupler $C2_{\#2}$ are shown in Figure 8. The abscissa A_1' of the lowest point of the resonant curve and the abscissa B_1' of the zero point of the demodulation curve completely coincide with each other. The linear region of the demodulation curve $|C_{11}'C_{12}'|$ is also symmetrical, that is, $|C_{11}'B_1'| = |B_1'C_{12}'|$. The center frequency of the laser is finally locked at the zero point of the demodulation curve. Thus, the center frequency of the laser can be accurately locked at the resonant frequency of the light wave. The experimental result is almost completely consistent with simulation result shown in Figure 4.

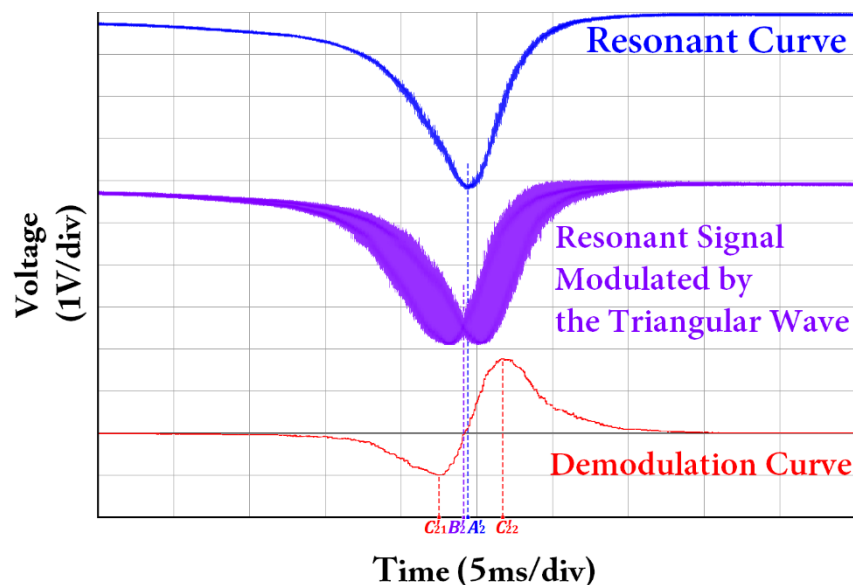


Figure 7. Measured resonant curve, resonant signal modulated by the triangular wave, and demodulation curve, when using coupler $C2_{\#1}$ connected to FRR.

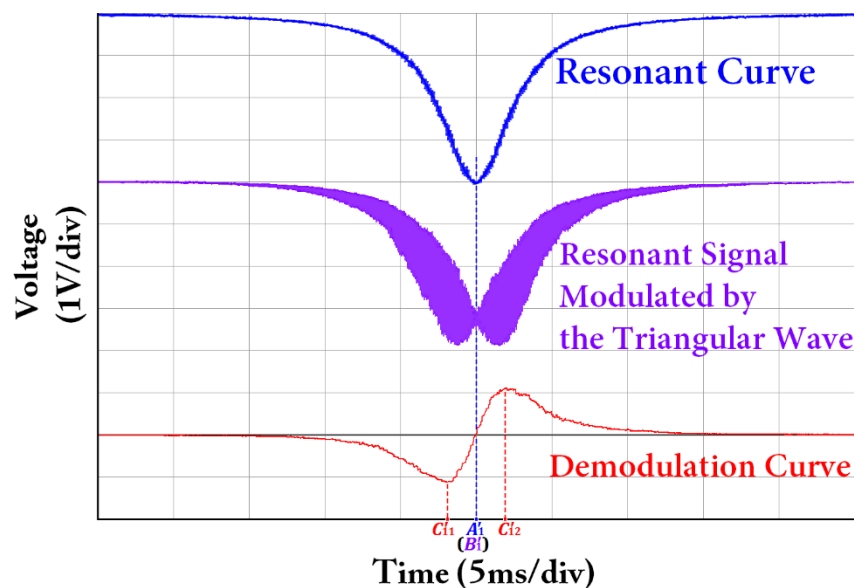


Figure 8. Measured resonant curve, resonant signal modulated by the triangular wave, and demodulation curve, when using coupler C2_{#2} connected to FRR.

5. Conclusions

Resonance asymmetry phenomenon in RFOG is found in the experiment. In this paper, a new mathematic model is established. The influence of the normal mode loss difference of the coupler (the phase difference between the coupler cross port output optical field and direct port is less than the ideal $\pi/2$) on the symmetry of the resonant curve, the resonant signal modulated by the triangular wave, and the demodulation curve are all analyzed in detail. At the same time, it is proved that the asymmetry of the resonant curve will lead to the asymmetry of the resonant signal modulated by the triangular wave and the demodulation curve from the theoretical simulation and the experiment. The resonant curve asymmetry will affect the system open-loop bias and its stability, which directly affects the angular velocity measurement accuracy. Therefore, the analysis of the factor that affects the symmetry of the resonant curve is of great significance to improve the sensitivity of the gyroscope.

Acknowledgments: Guangdong Provincial Natural Science Foundation of China (2015A030310464), and The Science & Technology Innovation Commission of Shenzhen (JSGG20150512162504354).

Author Contributions: Z.L. and N.H. conceived and designed the experiments; Z.L., N.H., X.S. and C.J. performed the experiments; X.W. and C.L. analyzed the data; C.L. contributed materials and analysis tools; Z.L., N.H. and X.W. wrote the paper.

Conflicts of Interest: The authors declare no conflict of interest.

References

1. Wang, L.; Zhang, C.; Gao, S.; Wang, T.; Lin, T.; Li, X. Application of Fast Dynamic Allan Variance for the Characterization of FOGs-Based Measurement While Drilling. *Sensors* **2016**, *16*, 2078. [[CrossRef](#)] [[PubMed](#)]
2. Meyer, R.E.; Ezekiel, S.; Stowe, D.W.; Tekippe, V.J. Passive fiber-optic ring resonator for rotation sensing. *Opt. Lett.* **1983**, *8*, 644–646. [[CrossRef](#)] [[PubMed](#)]
3. Liang, W.; Ilchenko, V.S.; Savchenkov, A.A.; Dale, E.; Eliyahu, D.; Matsko, A.B.; Maleki, L. Resonant microphotonic gyroscope. *Optica* **2017**, *4*, 114–117. [[CrossRef](#)]
4. Ciminelli, C.; Agostino, D.D.; Giuseppe, C.; Olio, F.D.; Conteduca, D.; Ambrosius, H.P.M.M.; Smit, M.K.; Armenise, M.N. A High-Q InP Resonant Angular Velocity Sensor for a Monolithically Integrated Optical Gyroscope. *IEEE Photonics J.* **2016**, *8*, 1–19. [[CrossRef](#)]

5. Olio, F.D.; Ciminelli, C.; Armenise, M.N.; Soares, F.M.; Rehbein, W. Design, fabrication, and preliminary test results of a new InGaAsP/InP high-Q ring resonator for gyro applications. In Proceedings of the International Conference on Indium Phosphide and Related Materials, Santa Barbara, CA, USA, 27–30 August 2012; pp. 124–127.
6. Qian, K.; Tang, J.; Guo, H.; Liu, W.; Liu, J.; Xue, C.; Zheng, Y.; Zhang, C. Under-Coupling Whispering Gallery Mode Resonator Applied to Resonant Micro-Optic Gyroscope. *Sensors* **2017**, *17*, 100. [[CrossRef](#)] [[PubMed](#)]
7. Ezekiel, S. Optical gyroscope options: principles and challenges. In Proceedings of the 18th International Optical Fiber Sensors Conference, Cancun, Mexico, 23–27 October 2006; p. MC1.
8. Jin, Z.; Yu, X.; Ma, H. Resonator fiber optic gyro employing a semiconductor laser. *Appl. Opt.* **2012**, *51*, 2856–2864. [[CrossRef](#)] [[PubMed](#)]
9. Ying, D.; Mao, J.; Li, Q.; Jin, Z. A miniaturized compact open-loop RFOG with demodulation signal compensation technique to suppress intensity modulation noise. *Opt. Commun.* **2016**, *359*, 364–371. [[CrossRef](#)]
10. Stokes, L.F. Effects of normal mode loss in dielectric waveguide directional couplers and interferometers. *IEEE J. Quantum Electr.* **1983**, *19*, 1888–1896.
11. Stokes, L.F. Single-Mode Optical Fiber Resonator and Applications To Sensing (Fiber Sensor, Fiber Laser, Fiber Gyroscope). Ph.D. Dissertation, Stanford University, Stanford, CA, USA, 1984.
12. Ebberg, A.; Lehnert, H. Effects of resonance asymmetries on the conversion of laser phase noise into amplitude noise in fiber optic ring-resonators. *IEEE Photonics Technol. Lett.* **1990**, *2*, 470–472. [[CrossRef](#)]
13. Chang, X.; Ma, H.; Jin, Z. Resonance asymmetry phenomenon in waveguide-type optical ring resonator gyro. *Opt. Commun.* **2012**, *285*, 1134–1139. [[CrossRef](#)]
14. Takahashi, M.; Tai, S.; Kyuma, K. Nondestructive measuring technique for misaligned angle in polarisation-maintaining fibre coupler. *Electron. Lett.* **1989**, *25*, 600–602. [[CrossRef](#)]
15. Lamouroux, B.; Prade, B.; Vinet, J.Y. Kerr effect in all-fiber cavities of optical gyros. *Appl. Opt.* **1990**, *29*, 750–753. [[CrossRef](#)] [[PubMed](#)]
16. Chen, Y.; Ma, H.; Jin, Z. Resonance asymmetry induced bias errors in waveguide type optical passive resonator gyro. *Appl. Opt.* **2012**, *51*, 2373–2378. [[CrossRef](#)] [[PubMed](#)]
17. Takahashi, M.; Tai, S.; Kyuma, K. Effect of reflections on the drift characteristics of a fiber optic passive ring resonator gyroscope. *J. Lightwave Technol.* **1990**, *8*, 811–816. [[CrossRef](#)]



© 2018 by the authors. Licensee MDPI, Basel, Switzerland. This article is an open access article distributed under the terms and conditions of the Creative Commons Attribution (CC BY) license (<http://creativecommons.org/licenses/by/4.0/>).